Three-dimensional optimization of penstock layouts for micro-hydropower plants using genetic algorithms

A. Tapia[*a], A. Rodríguez del Nozal[b], D. G. Reina[c], P. Millán[a]

[a]*Departamento de Ingeniería, Universidad Loyola. Sevilla (Spain)*
[b]*Departamento de Ingeniería Eléctrica, Universidad de Sevilla. Sevilla (Spain)*
[c]*Departamento de Ingeniería Electrónica, Universidad de Sevilla. Sevilla (Spain)*

Abstract

A Micro Hydro-Power Plant (MHPP) is a suitable and effective mean to provide electric power to rural remote communities without harming the environment. However, the lack of resources and technical training in these communities frequently leads to designs based of rules of thumb, compromising both the generation capacity and efficiency. This work makes an attempt to address this problem by developing a new tool to design the layout of MHPP. The proposed mechanism relies on a discrete topographic survey of the terrain and utilizes a Genetic Algorithm (GA) to optimize the installation layout, making it possible to explicitly incorporate requirements and constraints, such as power supply, cost of the installation, available water flow, and layout feasibility in accordance with the real terrain profile. The algorithm can operate in both single-objective mode (cost minimization) and multi-objective mode (cost minimization and power supply maximization), including in the latter Pareto dominance analyses. The algorithm is applied to a real scenario in a remote community in Honduras, obtaining good results in terms of generation capacity and cost reduction.

Keywords: micro-hydropower plants, genetic algorithms, optimization, renewable energy

1. Introduction

During the last decades, the positive effects of improving energy access on numerous factors such as health, education, economy and environment conservation, among others, have been proven. It is considered an efficient tool towards poverty eradication, leading developing countries towards a sustainable development [1, 2].

Despite of the fact that electrification is a significant goal for growth, around 800 million people still lacked access to electricity in developing countries in 2019, according to the World Data Bank [3]. Despite of the improvement achieved during the last years, a significantly negative impact has been recently caused in the energy marked due to the Covid-19 pandemic. In this context of crisis that is being faced by the government, pressure over utilities, electricity and other access providers has caused the increase of borrowing rates in countries with a large access deficit [4]. In this context, a crucial contribution to minimize the coverage of basic energy needs can be made by Renewable Energy Resources (RES). According to the Organization for International Co-operation and Development (OECD) [5], the share of renewable energies in electricity production has grown by a record of 2.3 % in 2020.

1.1. Renewable Energy Resources

In the next five years, electricity production from RES is expected to rise by almost 50%, to nearly 9,745 TWh. This is equal to the added demand of China and the European Union. Among the different RES alternatives, hydro-power remains as the primary source of renewable electricity generation. This is due to its high efficiency [6] and availability [7]: feasible hydropower estimated at almost 15,000 TWh/year is still present in the world today. It is relevant to note that new policies, oriented to encourage the installation and usage of renewable energy, are therefore evolving. For example, with the Environment & Energy Package 2030, the European Union has introduced a straightforward roadmap aimed at achieving a 32% rise in renewable energy integration and a 40% reduction in Greenhouse Gas (GHG) emissions compared to 1990 [8]. Also, the renewable energy sector could contribute to reactivate the current economic slowdown scenario affected by Covid-19 in these medium-term plans. By targeting remote and isolated areas, RES are even more important due to their ability to exploit isolated natural resources around the world. In this particular context, the role of Micro-Hydro Power Plants (MHPPs) is of especial relevance, as they constitute an efficient and affordable way to deal with traditional energy poverty scenarios [9, 10].

1.2. The challenge of optimizing MHPPs

The use of MHPPs is emerging as a decentralized source particularly used for meeting local energy demand. An introductory review of the different types of models and the most common techniques to evaluate the cost of hydro-power projects can be found in [11]. MHPPs are simple and robust installations with minimal equipment and labor requirements. This, together with its low cost and reduced environmental impact, makes this form of installation ideal for supplying remote communities

[*]Corresponding author
Email address: atapia@uloyola.es (A. Tapia[*])

with electricity, where the complexity of the land makes it difficult to link them to the main electricity grid [12]. These reasons have put MHPPs in the spotlight, becoming the subject of extensive studies by the scientific community and collaboration platforms during the last decades [13].

Despite of these advantages [14, 15], the design of MHPP installations for rural remote supply raises several challenges, especially given the context of poverty and lack of resources, which typically translates into sub-optimal systems. These issues are related to the complexity of the optimization problem that results of the design stages of a MHPP (such as choosing and sizing the equipment or finding the most adequate emplacement), and have been extensively discussed in the literature [16, 9, 17, 17].

A recurrent problem in this type of facilities is the increasing seasonal shortfall in electricity supply from standalone MHPP. In hot and dry seasons, the water flow is low, and consequently, the system cannot provide a high amount of power [18]. To overcome this limitation, hybrid installations that combine more than one renewable energy source are employed. For instance, in [19], solar and wind energies are introduced as complementary energy sources. In addition, in this study a cost analysis is performed. The analysis carried out in [20] intends to achieve a compromise between economic and environmental performance, when an MHPP shortfall is complemented by diesel generators, photo-voltaic plants, and energy storage systems. Although from an environmental point of view, hybrid systems are promising, the obtained results turn out that they are only economically viable for larger installations. Another alternative to increase the viability of these installations is using water distribution systems. The authors in [16] demonstrate that the cost of this installation can be noticeably reduced with the use of already existing infrastructures. In [21] a methodology to quantify the potential for hydro-power based on the excess energy in a water distribution network is proposed and applied to a real case.

Despite the variability in the power output of MHPP, these installations remain one of the best options for isolated areas without access to the main electricity grid. Therefore, and in order to increase its viability, many studies on the optimization of these installations have been carried out [9, 17, 22]. Two main problems are addressed in the literature on the optimization of MHPP installations: (i) on the one hand, the choice of the turbine, i.e. the selection of the head, runner diameter, etc (an interesting review of different types of turbines and their performance is presented in [9]), and (ii) the optimization of the layout, i.e. the design and location of the components that constitute the facility (an overview of micro-hydro systems is presented in [17], where some of their basic components like turbine and generator are explored). Moreover, a review of works assessing the impact and identifying escalating policy issues related to MHPP installations can be found in [22]. An interesting tool for MHPP design can be found in [23]. This tool analyzes and estimates the most important economic indices of an MHPP using the sensitivity analysis method. Furthermore, by comparing the technical, economic and reliability indexes, the proposed approach determines its optimal installation capacity.

When focusing on the optimization of the installation many approaches can be found [24, 25, 26]. For instance, in [24] a numerical model is developed in which the technical performance, energy production, maintenance and operational costs of a hydro-power plant are obtained for different proposed designs. In [27], an increase in the capacity of an existing hydroelectric plant is addressed. To do that, a new surge tank is built and the size of a diaphragm between the bottom of the new balance shaft and the race tunnel is optimized to ensure safe pressure in the race tunnel. Regarding the optimal operation of the hydroelectric power plant, in [28], the authors show how model predictive control can be used to overcome prediction errors in the available water in the reservoir and, therefore, improve the operation and the efficiency of the system.

Furthermore, the work in [26] presents the most important features of the turbine model from a control point of view. Various control methods are analyzed taking into account the complexity of the method, dynamics, adaptability and applicability. Other alternatives are based on optimizing existing installations to increase the potential power generation [25]. Some authors also propose to optimize the operation of the plant without a relocation of their components. For instance, in [29] the authors introduce a linear objective function as an alternative to a nonlinear form with the aim of maximizing hydro-power energy generation.

The aforementioned references reveal that the complexity of the problem, and generally, the difficulty of optimizing the installation designs using conventional gradient-based optimization strategies. For this reason, the use of computational intelligence approaches and their application to this kind of problems has gained great importance [30, 31, 32].

In [30], the authors develop a numerical optimization methodology, which is applied to a Turgo water turbine in order to find the best blade that maximizes the attainable hydraulic efficiency of the runner. The problem is solved with stochastic optimization using evolutionary algorithms. Other works use an evaluation algorithm that simulates in detail the plant operation during the year and computes its production results and economic indices [33]. The authors reveal that the optimal sizing in terms of economic benefits of the investment does not coincide with the one that maximizes exploitation of the hydraulic potential. Similarly, in [34] the jet-runner interaction of a Pelton turbine in various operation conditions is studied. In addition, a numerical design optimization of the bucket shape is performed. In this case, the authors employ a Lagrangian formulation and solve the problem using evolutionary algorithms. Moreover, [35] investigates the potential of using a proposed meta-heuristic method to provide optimal operations for multi-reservoir systems, with the aim of optimally improving hydropower generation. An interesting work can be found in [36], where the authors propose a theoretical analysis to find the optimal penstock for low head plants. This work is of especial relevance, given that it addresses the optimization problem from an elegant analytical approach, which requires a strong simplification of the problem geometry. In particular, the analysis draws from a 2D formulation of the MHPP layout, which, in

addition, is considered as a rectilinear segment. Despite of the elegance of the obtained result, there are some factors that limit its implementation. For example, a river profile with a highly irregular profile may differ too much from the model.

An improved approach can be found in [37], where a methodology is proposed to address the optimization problem considering any arbitrary 2D river profile. As the authors point out, this consideration increases the complexity of the problem and thus meta-heuristic approaches are suggested. Although this same strategy has been improved in later works [31, 32], none of them considers a precise 3D approximation of the river, which extremely affects the optimality of the installation.

This paper proposes a 3D formulation of the problem, and a Genetic Algorithm (GA) [38] to determine the optimal layout of the MHPP. To this end, the problem is stated as a constrained optimization problem that accounts for the generated power of the plant and its cost, including both the cost of the equipment and the civil works involved. The paper extends the previous work proposed by the authors in [31], where two-dimensional approximations of the river profile were considered. In this case, the novel formulation permits the consideration of the 3D terrain.

1.3. Contributions

This work proposes a novel strategy to address the optimization of an MHPP, by means of a formulation, to permit the explicit consideration of the real 3D terrain geography. This allows to make the most of the geographic particularities, such as river curvatures or cliffs.

It is also relevant to note that the methodology proposed constitutes a versatile framework for further applications in the optimization of MHPPs, enabling the consideration of additional elements (distribution grid, access or impassable or restricted areas) or its application to similar applications (road paths or piping systems).

The main contributions of this paper are:

- A novel three-dimensional approach is developed. This, in contrast to the two-dimensional approaches proposed in the literature, not only provides with better solutions that are not considered by the latter, especially in rivers with a high curvature, but also avoids errors that might appear when translating a 2D solution into the real 3D terrain.
- Development of a robust and efficient discrete formulation of the MHPP design problem to include the 3D terrain height map on a discrete basis.
- Development of a GA to determine the optimal layout of an MHPP, subjected to real topographical data of the MHPP emplacement. The proposed approach takes into consideration the power generated and the cost involved in equipment acquisition and civil works involved.
- Validation of the GA (in both single and multiobjective-mode) to design a MHPP in a real emplacement, using a piece of topographic data, including the comparison of the results with those obtained using a simplified, 2D-based simpler approach.
- Establishment of a a versatile framework for further applications in the optimization of MHPPs, enabling the consideration of additional elements (distribution grid, access or impassable or restricted areas) or its application to similar applications (road paths or piping systems).

The paper is organized as follows. First, Section 2 introduces the mathematical modeling of all the elements that constitutes the MHPP together with the corresponding cost terms and restrictions. Section 3 introduces the discretization of the terrain and the formal problem statement. In Section 4 the genetic algorithm proposed to solve the problem is presented. Finally, Section 5 presents and discusses the results obtained, and in Section 6 the main conclusions and further work lines are drawn.

2. Model of a MHPP

The working principle of a MHPP lies is the transformation of the potential energy of a natural water flow into electrical energy. This is done by extracting a portion of the flow and driving it downhill through a long pipe called penstock (see Fig. 1). This pipe is composed of a certain number of straight pipe segments, connected to each other by pipe elbows. These consist in heavy concrete blocks that are built in-situ at the ground level. At the end of the penstock, the kinetic energy of the flow is transformed into electrical energy by means of a generation unit, which consists of a water turbine and a generator. These elements are typically installed in a small building called powerhouse, placed besides the river, in such a way that the water flow is easily returned back to its natural course after exiting the turbine.

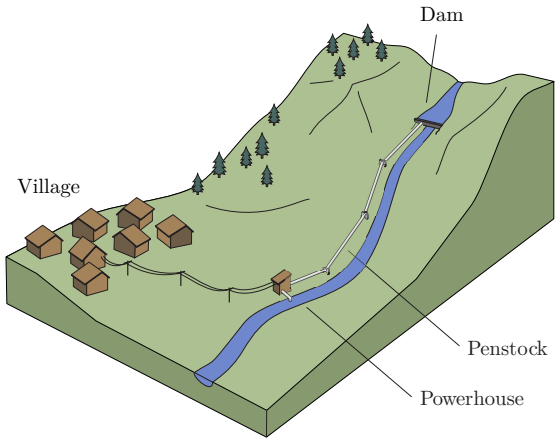

Figure 1: Basic scheme of a MHPP

It is relevant to note that, as only the dam and the powerhouse are required to be place along the river, an adequate 3D modeling of the terrain enables the penstock layout to save noticeable curves with straight segments, resulting in cheaper and

more efficient installations. This constitutes the main motivation of this work, and the challenging complexity increase with respect to the 2D approaches that have been traditionally addressed in the literature [32, 36].

There are two main variables that determinate the performance of the plant: the gross height of the installation, H_g, and the length of the penstock, L_p. In rough terms, a high gross height would allow a higher level of power generation, but a long penstock would imply a higher friction loss, and thus a decrease in the efficiency of the plant (and an increase of its cost). In addition, the diameter of the penstock, D_p, has a noticeable impact: the higher the diameter, the lower the losses due to friction, but the higher installation costs.

2.1. Layout of the plant

Let the terrain height profile be considered as a surface defined by a function $f(x, y)$ that, for a certain couple of latitude-longitude coordinates x, y, determines the topographic height $z = f(x, y)$ at that location.

The plant layout can be described as a set of ordered points, which in the developments to follow are referred as nodes, connected to each other on the x, y-map and defining the penstock deployment. Thus, the first and last nodes represent the location of the dam and the powerhouse, respectively, while the intermediate ones represent pipe elbows (angled connections between two consecutive straight pieces of the pipe).

Using this scheme, any arbitrary set of nodes, (x_i, y_i), from the x, y-map would represent a layout, defined by the broken line that connects them in ascending z-order (given that the penstock must have a non-negative slope). This layout can be parametrized by its arc-length as

$$\Delta(s) = \Big(\Delta_x(s), \Delta_y(s)\Big)$$

An example of a possible layout with 4 nodes has been represented in Fig. 2 for an arbitrary emplacement.

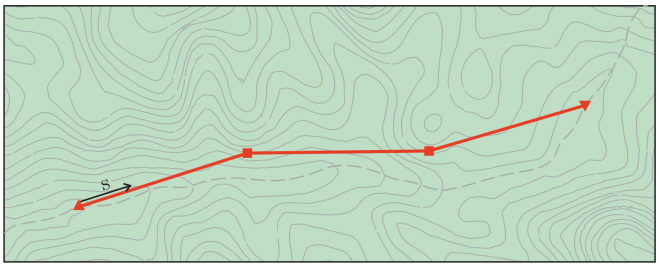

Figure 2: Example of a layout $\Delta(s)$ (red line) on an arbitrary terrain. The gray lines represent the contour height curves (continuous) and river (discontinuous). Note the location of the dam (▼), elbows (■) and powerhouse (▲) have been indicated.

Nevertheless, it is relevant to note that only those combinations whose end nodes (the emplacement of the dam and the powerhouse) are placed on the river would represent possible layouts. For this reason, the profile of the river on the map is also considered in the problem formulation, as will be discussed later.

On the other hand, although the nodes belong to the terrain surface, the penstock that results from their connection will not, and thus a certain gap between the penstock and the terrain is expected to be formed, which has implications on the civil works required.

2.2. Performance of the plant

The power delivered by the installation, P, can be determined by

$$P = \rho g Q H_t \eta, \tag{1}$$

where ρ represents the density of the water, g is the acceleration of gravity, Q the water flow rate, η the overall efficiency of the generation unit, and H_t the pressure head at the entrance of the turbine. It must be noted that, although the efficiency of the generation unit may vary greatly with its type and its operating regime, the consideration of a fixed piece of equipment to be installed, together with the power generation constraint translate into a very narrowed range for the efficiency.

Considering an action turbine, as the energy transformation is made at atmospheric pressure (a jet impacting the turbine wheel), all the energy is kinetic, and thus it can be written as

$$H_t = \frac{1}{2g} v^2 = \frac{1}{2g} \frac{Q^2}{S_{noz}^2}, \tag{2}$$

where S_{noz} is the cross sectional area of the nozzle injector. In an ideal case, this head pressure at the entrance of the turbine, H_t, is the same as the natural gross height, H_g. Nevertheless, due to the friction loss of the flow along the penstock, there is a non-negligible difference between these variables, and thus it can be written:

$$H_t = H_g - H_{loss} \tag{3}$$

The last term of (3) can be estimated by the summation of the distributed losses (friction along the inner walls of the pipe) and the concentrated losses (due to friction at each of the elbows and the nozzle).

$$H_{loss} = \left[\lambda \frac{L_p}{D_p} + \sum k_i + k_{noz} \frac{S_p}{S_{noz}}\right] \frac{1}{2g} \frac{Q^2}{S_p^2}, \tag{4}$$

being λ an experimental friction coefficient, L_p, D_p and S_p, the length, diameter and cross-sectional area of the penstock, respectively, k_i the concentrated loss coefficient due to pipe elbows and S_{noz} the cross-sectional area of the nozzle injector. Given the order of magnitude of a typical penstock [39], minor (local) losses are much inferior to major losses, and thus they can be neglected, resulting

$$H_{loss} \approx \frac{8\lambda}{\pi^2 g} \frac{L_p}{D_p^5} Q^2, \tag{5}$$

where the cross sectional area of the penstock, S_p, has been expressed in terms of its diameter, D_p, this is

$$S_p = \pi \frac{D_p^2}{4}$$

Following the approach in [31], the flow rate term Q can be isolated from (5) and substituted in (1), obtaining the power

generation in terms of the variables related to the installation layout (H_g, L_p, and D_p):

$$P = \frac{\eta\rho}{2c_D^2 S_{noz}^2}\left[\frac{H_g}{\frac{1}{2gc_D S_{noz}^2} + \frac{k_p}{D_p^5}L_p}\right]^{\frac{3}{2}} \tag{6}$$

2.3. Cost of the plant

The cost of the plant can be calculated as the sum of the costs of the generation unit, the powerhouse, the dam, and the penstock. Given the problem addressed in this work, i.e., finding the optimal installation layout, the first three terms are not expected to vary significantly. Therefore, the costs associated to the penstock are those to be optimized. These costs can be divided into the cost of the pipe itself, C_p, and the cost of the civil works related to its deployment on the terrain, C_{cw}. Thus, the total cost C (that will be expressed in cost units, c.u.) can be written as:

$$C = C_p + C_{cw} \tag{7}$$

2.3.1. Cost of the pipe

Traditional approaches typically consider that the pipe cost its proportionally to its length L and to the square of its diameter, D_p^2 [36, 40]. Besides, the cost of the pipe connections (elbows) can also be considered. Modeling these connections with equivalent costs, λ_c, in terms of virtual pipe segments has been demonstrated to provide good results [37]. However, in search of a more realistic approximation, polynomial dependencies, involving the pipe length, its diameter, and the number of elbows is used in this work:

$$C_p = L_p \sum_{i=0}^{m} a_i D_p^i + n_c \sum_{i=0}^{n} b_i D_p^i \tag{8}$$

where n_c represents the total number of pipe elbows of the penstock, and constants a_i and b_i are experimentally adjusted to fit the real costs from local manufacturers.

2.3.2. Cost of the civil works

Regarding the costs involved in the deployment of the penstock, the gaps formed between the straight penstock segments and the irregular terrain must be considered, given their impact on the cost of the civil works. On the one hand, when the gaps are positive, supports must be installed to avoid the pipe from flexing. On the other hand, when they are negative, a ditches must be excavated (see Fig. 3-a).

Let $\Gamma(s)$ be the linear interpolation of the nodes $(s, f(x_i(s), y_i(s)))$. Also, let $\gamma(s)$ be the height elevation of the layout $\Delta(s)$, this is

$$\gamma(s) = \Big(s, f(\Delta_x(s), \Delta_y(s))\Big)$$

The gap between the terrain and the penstock can now be written as the difference between $\Gamma(s)$ and $\gamma(s)$ (see Fig.3-b). To model the casuistry previously described, related to the nature of the gaps, two functions $\epsilon_{sup}(s)$ and $\epsilon_{exc}(s)$ are defined as

$$\epsilon_{sup}(s) = \begin{cases} \Gamma(s) - \gamma(s) & where\ \epsilon_{sup} \geq 0 \\ 0 & otherwise \end{cases}$$

$$\epsilon_{exc}(s) = \begin{cases} \gamma(s) - \Gamma(s) & where\ \epsilon_{sup} \leq 0 \\ 0 & otherwise \end{cases}$$

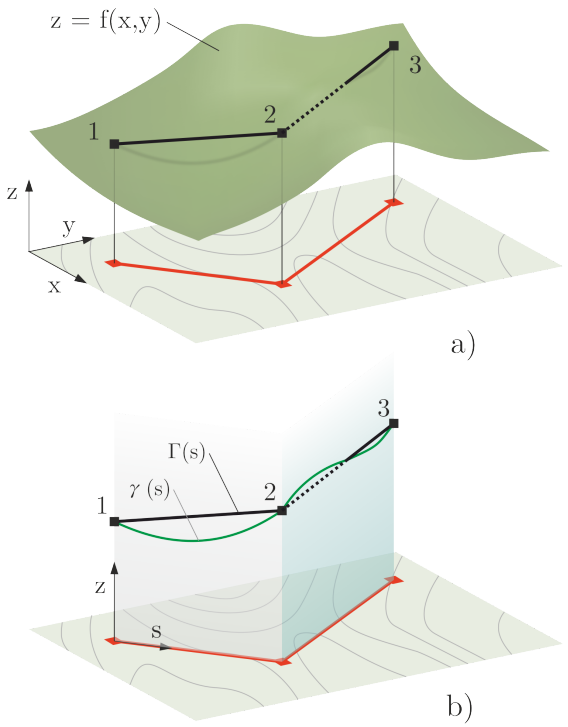

Figure 3: a) Illustration of two pipe segments where the formation of gaps is evidenced. The parts of the penstock above the ground (continuous line) requires the installation of supports, while those parts under the ground (dashed line) require excavations. b) Obtaining of functions $\Gamma(s)$ and $\gamma(s)$ in the space $s - z$.

Note that these expressions define the positive and negative values of the gap, respectively. With this in mind, the costs associated to the installation of the supports and the excavations can be written as:

$$C_{cw} = C_{sup} + C_{exc} \tag{9}$$

To compute the cost of the supports, C_{sup}, the linear density of supports required, μ_{sup}, is multiplied by the cost of each support and then integrated along the layout $\Delta(s)$. The cost of a single support can be approximated using a proper constant, k_{sup}, multiplied by the squared height (see Fig. 4-right), resulting in

$$C_{sup} = \mu_{sup} \int_{\Delta} \Big(k_{sup}\epsilon_{sup}\Big)^2 ds, \tag{10}$$

Note that an additional length, ϵ_0, is generally required in order to nail the support to the ground. This length will be considered as a certain fraction of ϵ_{sup}, and thus will be grouped in k_{exc}.

The cost proposed for the excavations is proportional to required excavation volume. Considering that a certain cut slope angle $\beta > 0$ might be required (depending on the properties of the terrain), a v-shaped cross section is proposed (see Fig. 4-left). The cost k_{exc} can thus be written as the cost of excavating a unit volume times the integral of the excavation section along the projected layout $\Delta(s)$, this is:

$$C_{exc} = k_{exc} \int_{\Delta} \left(tan\left(\beta_{exc}\right) \epsilon_{exc}^2 - D_p \epsilon_{exc} \right) ds, \tag{11}$$

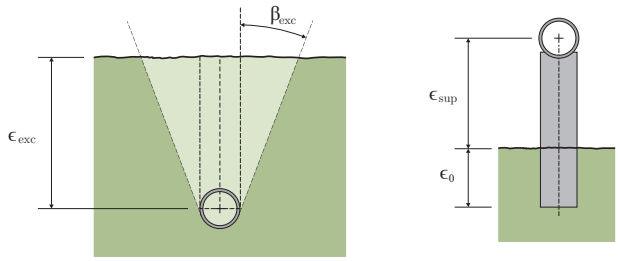

Figure 4: Scheme of excavations (left) and supports (right)

3. Problem formulation and discretization

On the basis of the proposed model, the optimization problem addressed is formulated as finding a distribution of nodes (and thus an MHPP layout X) that generates a required power supply, P_{min}, with the minimum cost, C:

$$\begin{aligned} \text{minimize} \quad & \text{C} \\ \text{s.t.} \quad & P > P_{min}, \end{aligned}$$

C and P can be determined using, respectively, expressions (7) and (6). Given the complexity of tacking this problem with a continuous analytic approach, a discretization strategy is developed to get a simpler and more efficient formulation.

3.1. Terrain

The height profile of the terrain under consideration, previously described through as the function $z = f(x, y)$, is approximated by the linear interpolation of a set of local height measurements, generally obtained by means of a topographic survey. These points build a $m \times n$ grid of data points T_i. Each of these points contains the spatial information, (x, y, z), of a topographic point of the terrain, and can be chosen to locate a pipe connection.

However, none of them can be chosen as emplacements for neither the turbine nor the dam, given that these two elements must be placed along the river profile. Therefore, the layout of the river is discretized in a similar way, resulting on a set of new points, R_i, containing also the corresponding topographic spatial information.

3.2. Plant layout

The layout of the MHPP is based on an extension of the one proposed in [37], from which certain important considerations must be taken. The proposed strategy consists of defining the layout of the plant by selecting a subset of S and T points, which will constitute the nodes of the layout, fulfilling the following:

1. The sequence of nodes are ordered by ascending topographical height, z, defining the order in which these are connected to each other.
2. The first node (the one at a lower topographical height) represents the powerhouse.
3. The last node (the one at a higher topographical height) represents the dam.
4. The rest of the nodes represent pipe elbows.

For a better understanding, an illustrative scheme of an arbitrary layout constituted for the following nodes:

$$X = \{R_8, T_{45}, R_6, T_{48}, R_3\} \tag{12}$$

is represented in Fig. 5. Note that, as long as the first and last nodes are chosen among R points (as the extraction and return of the water flow must be done on the river), both R and T points can take part in a layout. Given this sequence, the computation of the gross height, H_g, and the penstock length, L, is immediate.

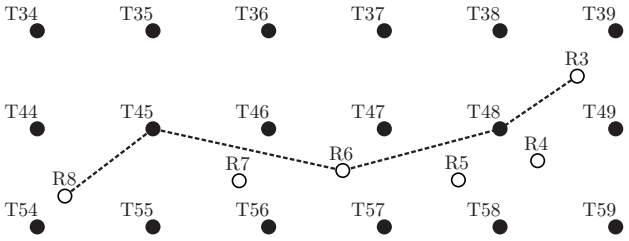

Figure 5: Scheme of a possible layout represented in dashed line. Terrain nodes (T) are represented in black and river nodes (R) in white. Note that, for this solution, points T_{45}, T_{48} and R_6 represent elbows of the penstock, while R_3 and R_8 represent, respectively, the location of the powerhouse and the location of the dam.

3.3. Complexity of the problem

The proposed plant layout design is a complex combinatorial problem. According to the nodes that can be used for the layout, the number of possible combinations is $2^{M \times N + S + 5}$, being $M \times N$ the number of terrain points, S is the number of river points, and 5 the number of bits used to code the diameter of the pipes. The actual number is lower since not all pairs of nodes can be connected due to terrain restrictions. It can be observed that the number of possible solutions grows exponentially with the number of considered points (terrain and river points). Finding a connected graph among the selected nodes that satisfies the restrictions would be a NP-complete problem. Moreover, finding the optimal cycle in the connected graph that

minimizes/maximizes cost and/or power is a NP-hard problem; consequently a brute force algorithm cannot be used. Thus, the utilization of a meta-heuristic approach like a GA is appropriate due to the complexity of the problem.

4. Genetic algorithm

Genetic Algorithms (GA) are meta-heuristic optimization algorithms that have been widely used to solve engineering problems [41, 42]. They are based on the Darwinian theory of evolution [43]. The main idea behind a GA is to encode a feasible solution in a chromosome-like structure, namely individual, where each gene represents an independent variable of the problem. Generally, the algorithm starts with a set of potential individuals or initial population. The genes of the individuals forming the initial population are chosen by a random process following a uniform distribution. Then, the initial population improves each generation by applying genetic operators, such as selection, crossover, and mutation. After a number of generations, the algorithm stops, and the best solution is determined.

4.1. Single objective case

In this work, a μ+λ version of GA is employed [44]. For this algorithm, the individuals (solutions) are codified in a chromosome-like structure, in which all the necessary variables are encoded. Fig. 6 shows the procedure to generate a new generation Gen_{t+1} in the GA from the current generation Gen_t. In this algorithm, a population of size μ is used, from which an offspring of size λ is generated at each generation. The offspring λ is generated through a selection, which is based on tournament selection (see more details later in this section), and the genetic operators, such as crossover and mutation. Both genetic operators are probabilistic operations. Therefore, a new individual contained in λ can be generated by crossing and/or mutating the parents selected from the μ individuals. Once the extended population is created with a size of $\mu + \lambda$ individuals, a new selection of μ individuals is conducted to obtain the new generation Gen_{t+1}. This strategy increases the elitism of the algorithm, as the new offspring must compete the parents to survive (see second selection in Fig. 6). The crossover and mutation probabilities define the exploration and exploitation capabilities of the GA. The optimal values are not universal; consequently, a fine tuning should be conducted (see Appendix B).

4.1.1. Individual representation

The representation of an individual or solution (see Fig. 7) uses binary variables associated to each of the candidate points for installing nodes ($n \times m$ variables δ for T points and s variables γ for R points). Note that T-nodes are sub-indexed by means of the corresponding row and column in the terrain grid. These variables are used in such a way that a node is installed at a certain point if the corresponding binary variable (gen) is 1, and it is not otherwise. In addition, the diameter of the pipe is embedded in the chromosome by using 5 bits, which allows encoding 32 decimal numbers to determine the value of the penstock diameter, D_p, in centimeters. Note that, as D_p cannot be equal to 0, the values represented are within the interval 1-32 cm.

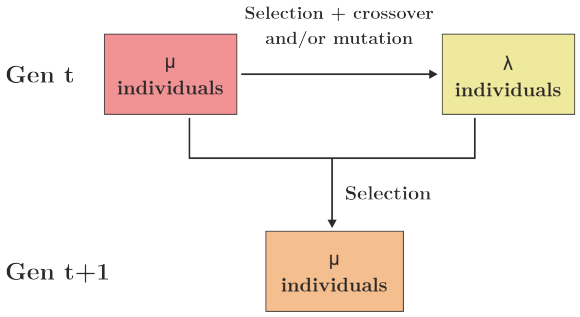

Figure 6: Functioning of $\mu + \lambda$ genetic algorithm

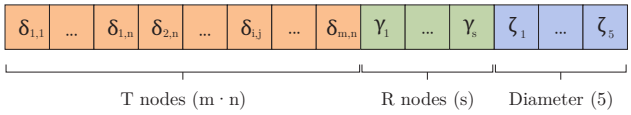

Figure 7: Chromosome structure

4.1.2. Initial population

The initial population is generated randomly. Nevertheless, given the complexity of the layout generation, which requires to fulfill conditions 1-4 in Section 3.2, it is unlikely to create feasible individuals using a random generation scheme. Therefore, a tailored generation algorithm is developed. The proposed approach is based on defining an oriented graph using the points T and R as nodes and connecting them as follows:

1. Neighboring nodes of type T are connected to each other (both horizontally and vertically) .
2. Consecutive nodes of type R are connected to each other following the river layout.
3. Each node of type R is connected to its 4 nearest neighboring nodes of type T.

For all the cited arcs or connections, the direction is always defined by the negative height gradient among the two connected nodes. That is, arcs are oriented in such a way that topographic height decreases. For the generation of every new individual, random weights are re-assigned to the arcs and the Dijkstra algorithm [45] is applied to find the shortest route connecting two nodes randomly chosen from the river (R nodes).

One example of an oriented graph obtained with this approach, applied to the example previously introduced, is shown in Fig. 8, where a possible individual is generated connecting nodes R_4 to R_7.

4.1.3. Fitness function

The fitness function is given by the cost of the plant, (7): the lower the cost, the better the solution is. Nevertheless, as invalid solutions must be discarded in order not to participate in the following generations of the GA, death penalty is used to penalize invalid individuals (these are individuals whose end

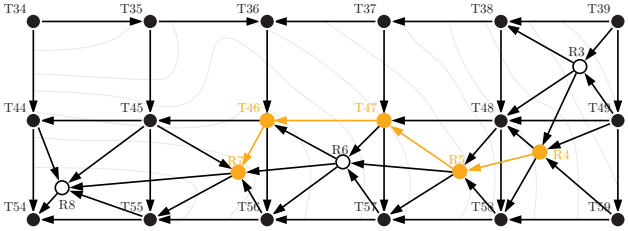

Figure 8: Graph generated for the individual generation scheme. Note that an example individual generated to connect node R_4 (dam) to R_7 (powerhouse) has been highlighted in orange.

nodes do not belong to the river). As a result, the fitness F of a solution is calculated as

$$\begin{cases} if & \textbf{solution valid} & F = (7), \\ & else & F = \infty. \end{cases} \tag{13}$$

4.2. Genetic operators

In this work, a tournament selection mechanism is used. This operator consists of randomly selecting a number of individuals that compete to each other to be chosen as parents. A tournament size of three individuals has been selected, given the good performance that it has demonstrated of most problems in the related literature [46].

A custom crossover technique has been implemented to improve the feasibility of the offspring generated at each generation. The proposed scheme consists of creating two individuals equal to the parents and then copy the gens with a value of 1 from one parent to the other with a certain probability μ_{cx}. This way, high values of μ_{cx} will result in descendants similar to an OR operation between the two parents, while low values will result in descendants similar to the parents. This scheme pursuits the creation of feasible individuals with competitive fitness values.

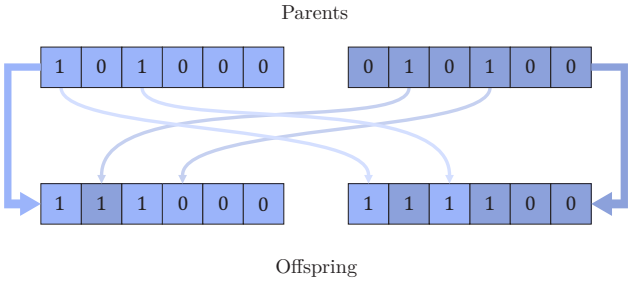

Figure 9: Scheme of the crossover operator

Regarding the mutation operator, three different operations have been considered in the scheme:

- With a certain probability, $p_{mut,10}$, each gene with value 1 can swap its logical value to 0.
- With a certain probability, $p_{mut,01}$, an arbitrary gene changes its value from 0 to 1.
- With a certain probability, $p_{mut,move}$, a gene swaps its positive value with a different gene, corresponding to an adjacent point in the terrain grid.

These particular schemes, schematically represented in Fig. 10, aim at improving the individuals by applying small variations to their layouts, that can translate into relevant changes in its fitness, especially regarding the influence of the nodes distribution on of the cost of the required civil works. For a better understanding of both the crossover and mutation operators, detailed flowcharts have been included in Appendix B.

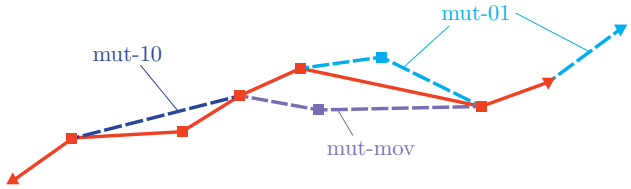

Figure 10: Example of the mutation schemes (dashed line) on an arbitrary individual (continuous line): Mutation mut-10 removes a node, mut-01 creates a new node and mut-mov swaps a node's position with a neighbour's.

4.3. Multi-objective case

In this case, the genetic algorithm is based on Pareto dominance. A solution is said to be dominated (according to the Pareto dominance) if and only if there is another solution that is strictly better in all considered objectives. In this work, the well-known NSGA-II algorithm has been used [47]. The main objective of NSGA-II algorithm is to find the Pareto front (solutions that are not dominated by others) in an efficient way. Fig. 11 shows the functioning of the NSGA-II. It uses the $\mu + \lambda$ structure to create an extended population through tournament selection and the genetic operators (crossover and mutation). Once the extended population is created, it is ordered (ranked) by the Pareto dominance. The first level of this ranking is composed of the dominant solutions, the second level is formed by solutions that are only dominated by the first level, and so on. The next step is to select the best μ individuals according to their dominance level. Notice that this selection is purely elitist; therefore, tournament selection is not used in this case. Furthermore, a distance metric is applied to the last dominance level that passes to the next generation. This distance metric guarantees diversity in the population. Thus, the resulting Pareto front is well distributed across the objective function limits (see more details in [47]).

4.3.1. Individual representation

The individual representation is the same that the used in the single-objective case (see Fig.7).

4.3.2. Fitness function

The fitness function used in the multi-objective case is computed as in the single-objective, but returning a tuple with both costs: C and power P values. This is

$$\begin{cases} if & \textbf{solution valid} & F = (7), (6) \\ & else & F = \infty, -\infty. \end{cases} \tag{14}$$

Please note that, in the case of unfeasible individuals (unfeasible solutions, whose end nodes do not belong to the river),

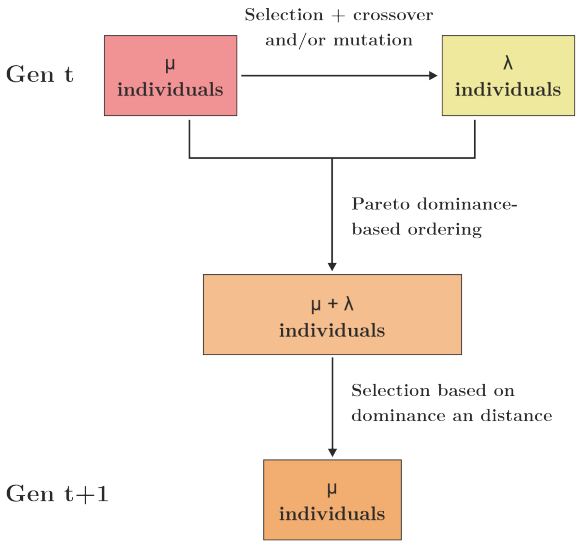

Figure 11: Functioning of NSGA-II

the death penalty is applied to both objectives. Consequently, these invalid individuals do not participate in the genetic operations.

4.4. Genetic operators

The crossover and mutation schemes used in Section 4.1 are employed.

5. Simulation results and discussion

This section presents the application of the proposed GA to a real-scenario problem. An aerial topographic survey was first employed to generate a piece of topographic data, conformed by a mesh of $m \times n = 2900$ T points and $s = 59$ R points. The parameters chosen for the problem are summarized in Appendix Appendix A

5.1. Single objective case

The MHPP is designed using a GA with the generation, crossover and mutation routines proposed. The simulator [1] has been developed using Python and DEAP[2]. The main parameters of its implementation are summarized in Table 1. The stopping criterion of the GA is the number of generations.

To tune the hyper-parameters related to crossover and mutation schemes, a greedy algorithm has been used. The results of the hyper-parametrization can be found in Appendix A. After the tuning process, the most successful combination of hyper-parameters was determined as:

$$\mu_{cx} = 0.6, \quad p_{mut,mov} = 0.01, \quad p_{mut,10} = 0.05, \quad p_{mut,10} = 0.20$$

In addition, these hyper-parameters provided a good convergence, as can be seen in Fig. 12, where the best fitness values obtained for each generation are represented.

[1]The code is available in [48]

[2]https://deap.readthedocs.io/en/master/

Table 1: Parameters of the single-objective GA

Parameter	**Value**
λ	2000
μ	2000
Generations	100
Selection	Tournament size = 3
Crossover	Custom crossover scheme
	$p_{cx} = [0.2, 0.3, 0.4, 0.5, 0.6, 0.7]$
	$\mu_{cx} = [0.20.40.50.60.8]$
Mutation	Custom mutation scheme
	$p_m = [0.80.7, 0.6, 0.5, 0.4, 0.3.]$
	$p_{mut,mov} = [0.01, 0.05, 0.10, 0.20]$
	$p_{mut,10} = [0.01, 0.05, 0.10, 0.20]$
	$p_{mut,01} = [0.01, 0.05, 0.10, 0.20]$
Number of trials	10
Diameter range	1-33cm

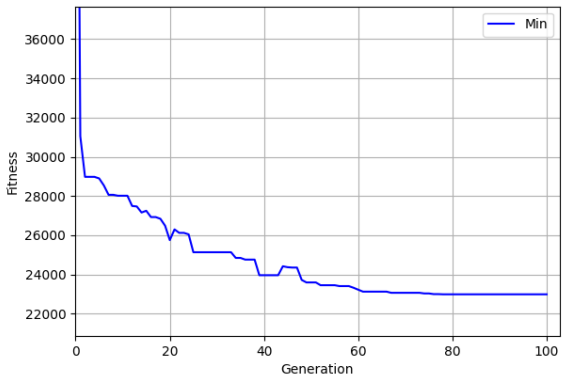

Figure 12: Best fitness value over generations obtained for the optimal combination of parameters.

The best solution obtained is an MHPP that generates 8.06 kW using a 15 cm diameter penstock, with a length of 521.49 m and a total of 8 elbows. This layout has been represented in Fig. 13, together with a height-map graph of the terrain, for a better understanding. Observing Fig. 13, it can be seen that the 3D approach allows cutting through rough terrain without requiring the layout to adapt to the sinuous curve of the river, which constitutes the main advantage of this approach with respect to traditional approaches which consider a 2D approximation of the river profile. To validate this hypothesis, this same problem is addressed in the next section by using a 2D-based, simplified approach.

5.1.1. Comparison with 2D-based simplified approach

In this section, the problem proposed is addressed by using the 2D-based algorithm from [31], which exclusively considers the river points (defined as R points in this work) to calculate the optimal layout. This 2D approach, which strongly reduces the computational complexity of the problem, is appropriate for

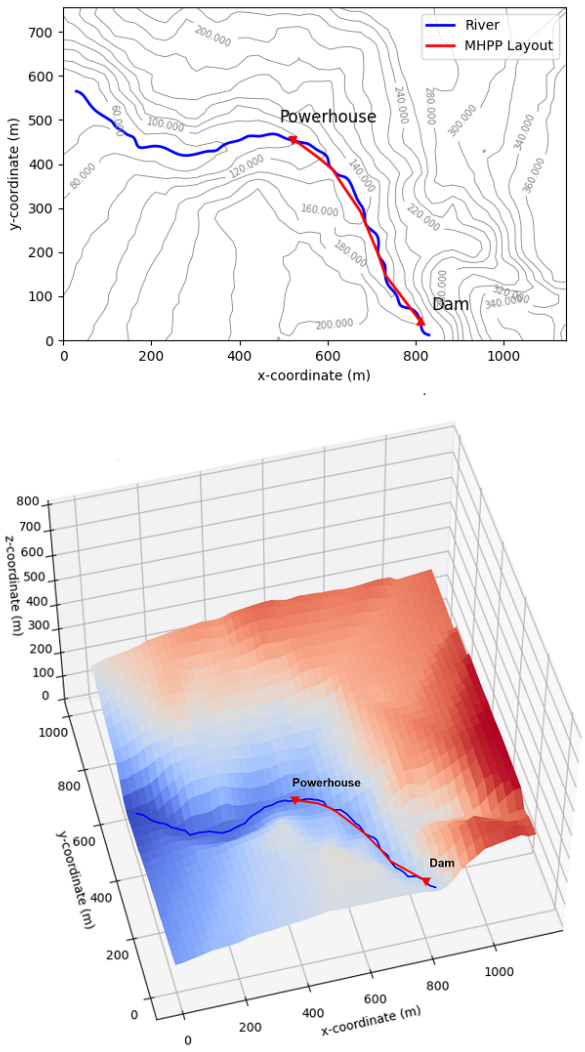

Figure 13: Orthographic (top) and 3D (bottom) representation of the optimal solution obtained

rivers with low or negligible curvature, where cutting off terrain does not provide a significant advantage on the deployment of a MHPP.

The algorithm has been applied using the same parameters from Table A.5. Also, a *mu-plus-lambda* scheme has been considered, with μ=λ=2000, through a total of 100 generations.

In Table 2, the relevant variables corresponding to the optimal solution obtained have been summarized. It can be seen that the 3D-based approach provides a noticeably better (14.7% cheaper) solution. This evidences the main advantage of the 3D approach, which can be better understood by representing the solution of the 2D approach. Also, from Fig. 15, it can be easily seen that the 2D method tends to introduce unnecessary complexities in the layout in those regions with high curvature, thus leading to sub-optimal solutions. Furthermore, it is interesting to note, though, that the solution obtained through the 2D approach provides a higher power output, exceeding the minimal requirement by a 11% (8.881 kW) while the solution obtained by the 3D approach only exceeds a 0.7% (8.056 kW). This oversizing is comprehensible given the narrower search space of the 2D approach, where only 2^{S+5} combinations are possible, instead of the $2^{(M\times N+S+5)}$ combinations that are considered in the 3D approach. Nevertheless, for a fair comparison, an additional simulation of the 3D algorithm has been performed to find the optimal solution to supply the 8.881 kW output obtained using the 2D approach. The results, summarized in Table 3 show that the same power output can be obtained at a 7% lower cost.

Table 2: Comparison of optimal solutions obtained for a 8 kW output with 2D and 3D-based approaches.

Approach	2D [31]	3D
Power output required (W)	8000	8000
Gross h. (m)	78.57	79.47
Power (W)	8880.93	8055.57
Pens. length (m)	534.11	521.49
Elbows	12	8
Pipe diam. (cm)	17	15
Cost (c.u.)	**26963.16**	**22989.09**

Table 3: Optimal solution obtained for a 8.881 kW output using the 3D-based approach.

Approach	3D
Power output required (W)	8880.93
Gross h. (m)	86.15
Power (W)	8894.34
Pens. length (m)	568.82
Elbows	9
Pipe diam. (cm)	15
Cost (c.u.)	**25035.44**

Also, it is relevant to highlight that all the possible solutions of the 2D approach are also possible solutions of the 3D approach, and thus the former would lead, in the best case, to the same solution of the latter.

5.2. Multi-objective case

A deeper analysis of the MHPP emplacement and its potential can be obtained by means of a multi-objective approach. To this end, an NSGA-II algorithm has been considered for a total of 2000 generations. Also, the optimal set of hyper-parameters obtained for the SO mode have been used. The rest of the relevant parameters are summarized in Table 4

The final population constitutes the Pareto front, which has been represented in Fig. 16-top. It can be seen that, for a large range of power values, the Pareto front has a linear tendency (included in the cited figure), whose slope can be understood as a marginal cost, this is, the cost increment that is necessary to produce a unitary increase in the power output. Using least squares, a linear model can be fitted to the individuals with

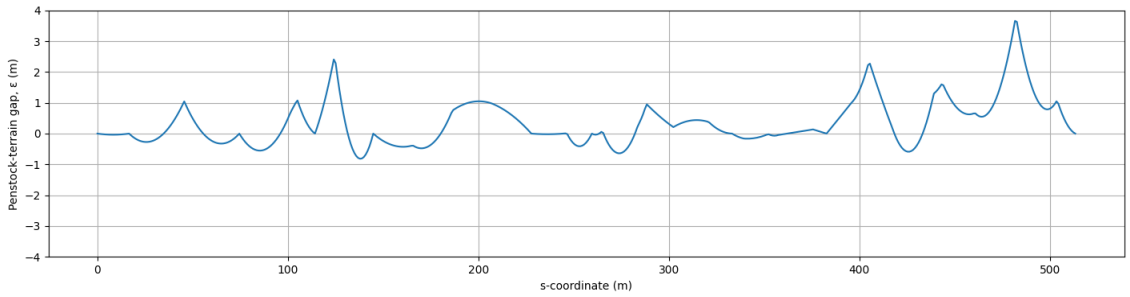

Figure 14: Penstock-terrain gap, ε, corresponding to optimal solution

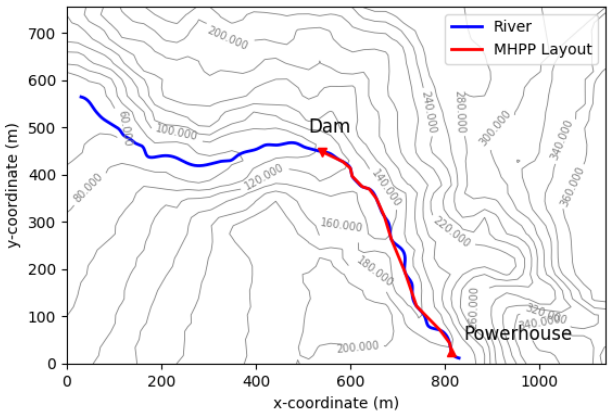

Figure 15: Representation of the optimal solution obtained using the 2D-based, simplified approach from [31]

Table 4: Parameters of the multi-objective GA

Parameter	**Value**
λ	2000
μ	2000
Generations	2000
Selection	NSGA-II
Crossover	Custom crossover scheme
	$p_{cx} = 0.7$
	$\mu_{cx} = 0.6$
Mutation	Custom mutation scheme
	$p_m = 0.3$
	$p_{mut,mov} = 0.01$
	$p_{mut,10} = 0.05$
	$p_{mut,01} = 0.20$
Diameter range	1-33cm

power values up to 20 kW, resulting in the following expression:

$$C = 3054.07P + 2475.20,$$

being C the cost expressed in c.u. and P the power in kW. This last expression constitutes a powerful tool to evaluate the potential of the emplacement and assist the first stages of design of the MHPP in accordance with variable budget constraints.

The linear tendency that observed in the Pareto front deserves specific attention, and thus, for the sake of a further analysis, the most relevant variables of the solutions from the Pareto front have been represented in Fig. 16-bottom.

First, it must be noted that a power output increase can be obtained (see expression (6)) by either increasing the diameter of the penstock, D_p, or the gross head, H_g, which generally requires an increase in the penstock length, L_p. If an approximately constant relation between these last variables, H_g and L_p, can be considered (that is, assuming an average slope of the river), it can be seen from expressions (6) and (8) that, if friction losses are low, both the cost and the power output increase approximately in the same proportion when the penstock length increases. This means that the marginal cost of increasing the power by extending the penstock is constant. On the other hand, this does not happen when the diameter is increased, as the cost increases more rapidly than the power, resulting in an increasing marginal cost.

This said, observing Figure 16-b it can be seen that, for the linear part, the penstock diameter, D_p, does not vary significantly, while from Figure 16-c the penstock length, L_p, is observed to increase proportionally, which explains the linear nature of the Pareto front. Also, it can be seen how the hypothesis of an average constant slope of the river is clearly not satisfied when power reaches values about 17 kW. At this point, the length of the penstock is such that it cannot be extended without occupying worse areas (note the sudden decrease in the average slope of the layout) of the river, and thus additional length is required to reach the required gross height (note the increase in Fig. 16-c). Also, this translates into higher friction loss, and thus an additional gross height is required to overcome it (note the increase in Fig. 16-d).

It is also relevant to highlight the presence of a vertical asymptote for high values of the generated power. This can be easily understood since the maximum power achievable is limited by the maximum gross height of the plant (note the saturation of H_g in the right part of the Pareto front). Those layouts, which make the most of the height difference along the river, can only be improved (in terms of power generation) by either (i) reducing the length (and thus the friction) of the pipe by cutting off rough terrain (at the expense of rapidly pushing up the cost of the excavations and supports, given (9), (10) and

(11)) or (ii) increasing the penstock diameter (with strongly increases the price of the pipe, given (8)). This can be evidenced by analyzing the evolution of the different variables in Fig. 16-b to -e.

It can be noted that this asymptote appears as a consequence of the finite portion of river considered in the topographic survey, as the algorithm is not capable of exploiting a larger range of the river to find better individuals. This means that these solutions do not necessarily represent optimal solutions if the portion of the river considered can be increased by using a new survey. In other words, the larger the portion of river considered, the higher the power value at which the asymtote appears, and as a practical conclusion, the portion of the river under study should be high enough to let the asymptote be formed outside the power values under study.

6. Conclusions

This article proposes a GA to address the problem of designing a run-off-the-river MHPP in emplacements with highly sinuous rivers, where the traditional 2D approach is not efficient. The proposed GA is built on a combinatorial basis by using a set of topographic data points, which are considered candidates for the emplacements of the different elements of the layout.

Using a simple hydraulic model of the MHPP, the optimization problem is formulated as minimizing the cost of the plant, subject to satisfying a certain power supply demand. The cost of the plant includes both the variable cost of the material and the civil works. These last parameters are calculated in terms of the layout and the terrain height map, in such a way that both excavations and supports are considered to its deployment.

Given the problem complexity, a tailored generation scheme is proposed to generate feasible individuals. In addition, both custom mutation and crossover operators have been developed to improve the exploration and intensification capabilities of the GA, while minimizing the probability of creating unfeasible individuals.

To validate the approach, a piece of topographical data from a real emplacement has been successfully applied to design a 8kW MHPP. This same problem has been solved using a 2D-based, simplified method proposed in the literature, resulting in a 14.7% cost reduction with the proposed approach. Although the narrower search space of the 2D approach caused an optimal solution with a noticeably higher power output over the required value (11%), an additional simulation of the 3D method provided a most economical (7% lower) solution that generates this same output.

simplified approach Given the noticeably higher power generated In addition, a multi-objective approach has been applied to obtain the Pareto front, which provides a better insight of the hydraulic potential of the emplacement.

In sight of the good results obtained, a continuation of the research is proposed to increase the versatility of the methodology that has been developed. First, the consideration of a more accurate model of the system is proposed. Additional variables such as the type of turbine installed, an accurate efficiency estimation or the costs of the distribution grid are expected to increase the reliability of the approach, at the expense

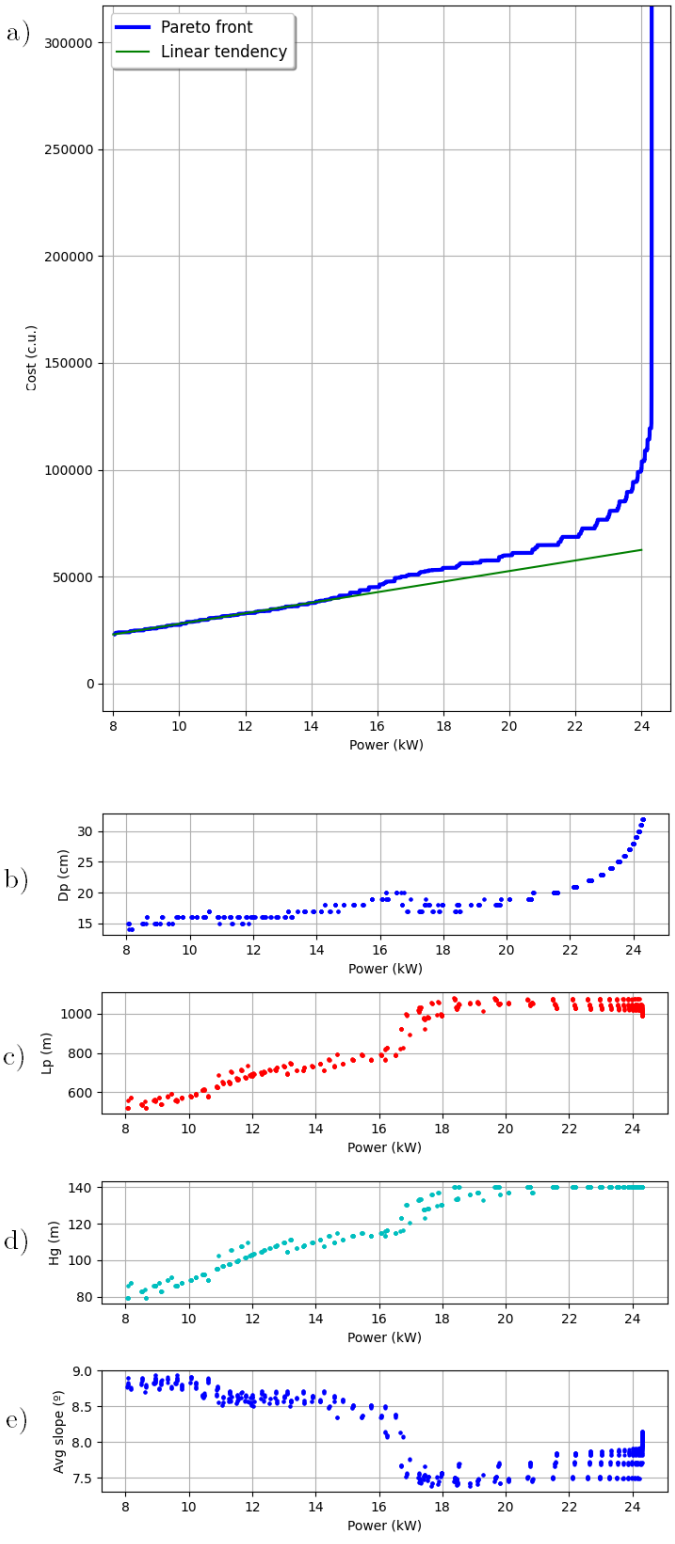

Figure 16: Representation of the Pareto front (a) and the relevant variables of its individuals (b-e).

of increasing the complexity of the problem, which would require a reformulation of the algorithm. Also, the possibility of developing a continuous approach that does not depend on candidate points but on arbitrary emplacements along the surface is considered a potential improvement to avoid that could lead to better solutions.

Acknowledgements

This research did not receive any specific grant from funding agencies in the public, commercial, or not-for-profit sectors.

Appendix A. Case study description and parameters

The case study considered is located in the rural village of San Miguelito, which was chosen based on a precise survey that included several visits to different potential communities. San Miguelito is a small rural community that belongs to the town of Quimistán in the north section of Santa Bárbara (Honduras). Due to its particularly remote location (until 2014, vehicle access was not possible), it has been excluded from the benefits of the national electrification grid, and given its environmental characteristics, it constitutes an ideal location for a MHPP due to the presence of an approachable natural stream. A minimum generation of 8 kW was established as the power required for the community.

The problem constants have been adjusted to fit the particular emplacement of the case study. In particular, the cost constants a_i and b_i have calculated to properly fit the average costs obtain from a local open repository [49]. All the required constants are summarized in Table A.5. Note that only the terms corresponding to the coefficients a_i and b_i indicated in this table take part in the cost expression.

Table A.5: Parameters of the problem

Parameter	Value
P_{min} (kW)	8
D_{noz} (mm)	22
K_{tub} (c.u.)	300
K_{sup} (c.u.)	130
K_{exc} (c.u./m^3)	100
X_{sup} (1/m)	0.2
β_{exc} (°)	10
a_0 (c.u./m)	13.14
a_1 (c.u./m^2)	99.76
a_2 (c.u./m^3)	616.10
b_0 (c.u.)	50
b_3 (c.u./m^3)	1200

Appendix B. Genetic algorithm operators and tuning

This section includes additional information of the genetic algorithm developed, together with the hyper-parameter tuning carried out for the genetic operators of the GA. In Figs. B.17 and B.18, both the crossover and mutation schemes are explained by means of a flowchart, for a better understanding.

Regarding the hyper-parameter tuning, the different combinations of mutation and crossover probabilities, p_{cx} and p_{mut}, have been tested through independent simulation routines of 10 trials each, while μ_{cx}, $p_{mut,mov}$, $p_{mut,10}$ remained fix at their reference values:

$$\mu_{cx} = 0.5, \quad p_{mut,mov} = p_{mut,10} = p_{mut,01} = 0.05$$

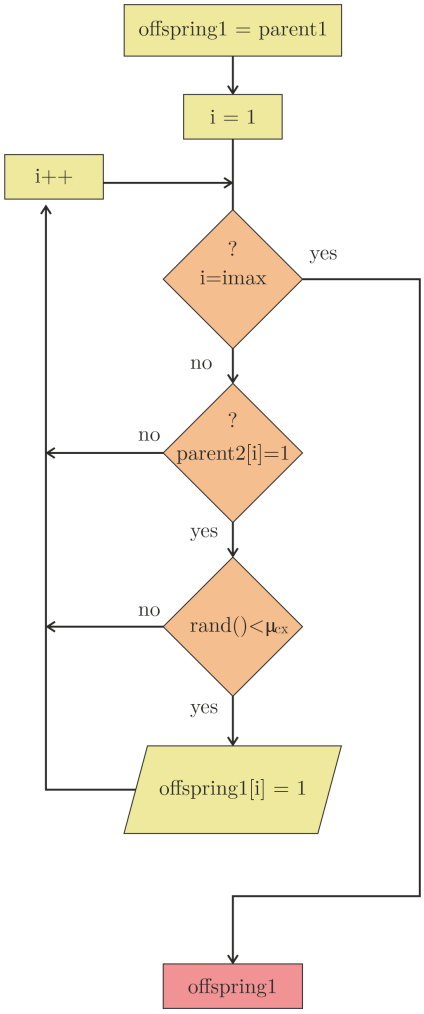

Figure B.17: Detailed flowchart of the crossover operator scheme for a single offspring. Note that the other offspring is created by an analogous operation.

The results obtained for the different combinations of mutation and crossover probabilities are summarized in Table B.6. It can be seen that 5 out of the 6 combinations led to the same optimal solution. Nevertheless, it can be observed that the standard deviation in the final population increases for high p_{mut} and low p_{cx} values. Thus, the first combination (p_{cx} = 0.70, p_{mut} = 0.30) was considered as the most adequate.

Once both the optimal crossover and mutation probabilities have been determined, the optimal value for μ_{cx}. The results obtained to tune this parameter are summarized in Table B.7. These results evidence that a value of μ_{cx} = 0.60 provides the best individuals, despite of the small differences among the

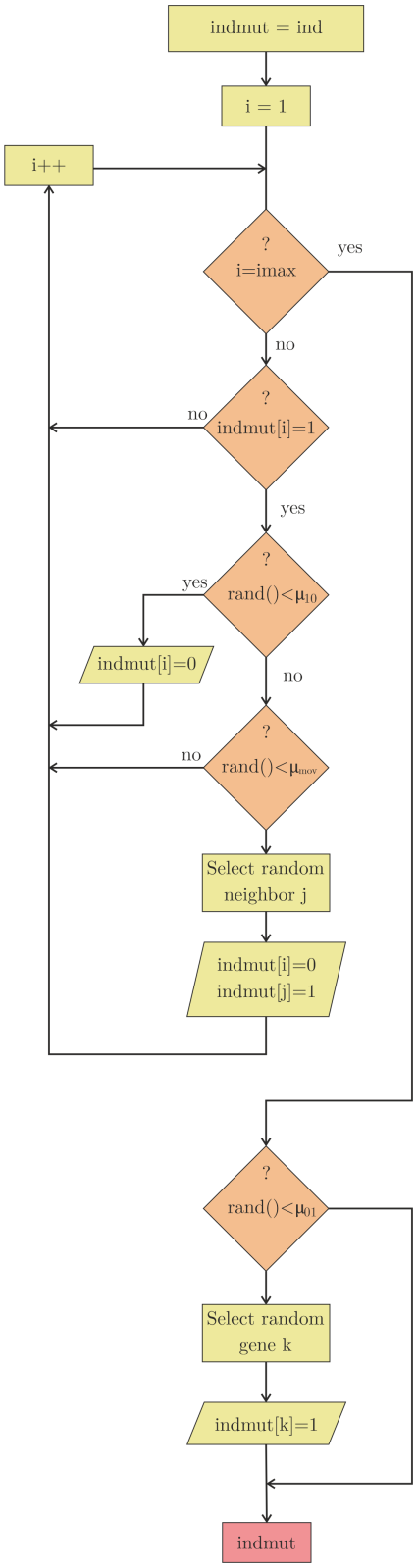

Figure B.18: Detailed flowchart of the mutation operator scheme.

tested values. Therefore, it suggests that the results of the GA have a low variability with respect to this parameter.

After the optimal value of μ_{cx} is determined, the values of the mutation hyper-parameters are determined in order. In Table B.8 the results of the tests proposed for $p_{mut,mov}$ are summarized. The lowest value proposed, $p_{mut,mov} = 0.01$ led to the optimal solution with the lowest standard deviation.

Finally, the results of the tests proposed to tune the hyper-parameters $p_{mut,10}$ and $p_{mut,01}$ have been summarized in Tables B.9 and B.10, respectively.

References

[1] M. Kanagawa, T. Nakata, Assessment of access to electricity and the socio-economic impacts in rural areas of developing countries, Energy policy 36 (6) (2008) 2016–2029.

[2] A. Okada, Poverty and education, Series International Development. Nippon-Hyoron-Sha Co., Ltd., Tokyo (in Japanese) (2004).

[3] The World Bank, Access to electricity, data retrieved from World Development Indicators, `https://data.worldbank.org/indicator/EG.ELC.ACCS.ZS` (2019).

[4] S. E. Hosseini, An outlook on the global development of renewable and sustainable energy at the time of covid-19, Energy Research & Social Science 68 (2020) 101633.

[5] I. E. Agency, Renewables 2020, 2020. `doi:https://doi.org/https://doi.org/10.1787/c74616c1-en`.
URL `https://www.oecd-ilibrary.org/content/publication/c74616c1-en`

[6] J. Kaldellis, K. Kavadias, Laboratory applications of renewable energy sources, Stamoulis, Athens (2000).

[7] K. Kaygusuz, Hydropower and the world's energy future, Energy Sources 26 (3) (2004) 215–224.

[8] Climate action, 2030 climate & energy framework.

[9] C. Jawahar, P. A. Michael, A review on turbines for micro hydro power plant, Renewable and Sustainable Energy Reviews 72 (2017) 882 – 887. `doi:https://doi.org/10.1016/j.rser.2017.01.133`.
URL `http://www.sciencedirect.com/science/article/pii/S1364032117301454`

[10] O. Paish, Small hydro power: technology and current status, Renewable and sustainable energy reviews 6 (6) (2002) 537–556.

[11] S. Mishra, S. Singal, D. Khatod, Optimal installation of small hydropower plant. a review, Renewable and Sustainable Energy Reviews 15 (8) (2011) 3862–3869.

[12] C. J. Blanco, Y. Secretan, A. L. A. Mesquita, Decision support system for micro-hydro power plants in the amazon region under a sustainable development perspective, Energy for sustainable development 12 (3) (2008) 25–33.

[13] A. Elbatran, O. Yaakob, Y. M. Ahmed, H. Shabara, Operation, performance and economic analysis of low head micro-hydropower turbines for rural and remote areas: a review, Renewable and Sustainable Energy Reviews 43 (2015) 40–50.

[14] A. Ranzanici, Sustainability comparison between endev and not-endev micro-hydro power (mhp) in indonesia: Analysis of the long-term technical, social, environmental and economic sustainability of the rural energy infrastructure of mhp in indonesia (2013).

[15] A. Gurung, O. P. Gurung, S. E. Oh, The potential of a renewable energy technology for rural electrification in nepal: A case study from tangting, Renewable Energy 36 (11) (2011) 3203–3210.

[16] A. Berrada, Z. Bouhssine, A. Arechkik, Optimisation and economic modeling of micro hydropower plant integrated in water distribution system, Journal of Cleaner Production 232 (2019) 877 – 887. `doi:https://doi.org/10.1016/j.jclepro.2019.06.036`.
URL `http://www.sciencedirect.com/science/article/pii/S0959652619319894`

[17] S. Anaza, M. Abdulazeez, Y. Yisah, Y. Yusuf, B. Salawu, S. Momoh, Micro hydro-electric energy generation-an overview, American Journal of Engineering Research (AJER) 6 (2) (2017) 5–12.

[18] A. Kuriqi, A. N. Pinheiro, A. Sordo-Ward, L. Garrote, Flow regime aspects in determining environmental flows and maximising energy production at run-of-river hydropower plants, Applied Energy 256 (2019) 113980.

[19] S. Hoseinzadeh, M. H. Ghasemi, S. Heyns, Application of hybrid systems in solution of low power generation at hot seasons for micro hydro systems, Renewable Energy 160 (2020) 323 – 332. doi:https://doi.org/10.1016/j.renene.2020.06.149.
URL http://www.sciencedirect.com/science/article/pii/S0960148120310715

[20] W. Apichonnabutr, A. Tiwary, Trade-offs between economic and environmental performance of an autonomous hybrid energy system using micro hydro, Applied Energy 226 (2018) 891 – 904. doi:https://doi.org/10.1016/j.apenergy.2018.06.012.
URL http://www.sciencedirect.com/science/article/pii/S030626191830881X

[21] I. Samora, P. Manso, M. J. Franca, A. J. Schleiss, H. M. Ramos, Energy recovery using micro-hydropower technology in water supply systems: The case study of the city of fribourg, Water 8 (8) (2016) 344.

[22] S. Kelly-Richards, N. Silber-Coats, A. Crootof, D. Tecklin, C. Bauer, Governing the transition to renewable energy: A review of impacts and policy issues in the small hydropower boom, Energy Policy 101 (2017) 251 – 264. doi:https://doi.org/10.1016/j.enpol.2016.11.035.
URL http://www.sciencedirect.com/science/article/pii/S0301421516306401

[23] S. Hosseini, F. Forouzbakhsh, M. Rahimpoor, Determination of the optimal installation capacity of small hydro-power plants through the use of technical, economic and reliability indices, Energy Policy 33 (15) (2005) 1948 – 1956. doi:https://doi.org/10.1016/j.enpol.2004.03.007.
URL http://www.sciencedirect.com/science/article/pii/S0301421504000679

[24] V. Yildiz, J. A. Vrugt, A toolbox for the optimal design of run-of-river hydropower plants, Environmental modelling & software 111 (2019) 134–152.

[25] R. Marliansyah, D. N. Putri, A. Khootama, H. Hermansyah, Optimization potential analysis of micro-hydro power plant (mhpp) from river with low head, Energy Procedia 153 (2018) 74–79.

[26] D. Borkowski, M. Majdak, Small hydropower plants with variable speed operation—an optimal operation curve determination, Energies 13 (23) (2020) 6230.

[27] F. Hachem, C. Nicolet, R. Duarte, G. De Cesare, G. Micoulet, Hydraulic design of the diaphragm's orifice at the entrance of the surge shaft of fmhl pumped-storage power plant, in: Proceedings of 35th IAHR world congress, TPU, 2013, pp. 1–12.

[28] R. Payet-burin, M. T. Kromann, S. Pereira-Cardenal, K. M. Strzepek, P. Bauer-Gottwein, Using model predictive control in a water infrastructure planning model for the zambezi river basin, in: 38th IAHR World Congress: Water–Connecting the World, CRC Press, 2019, pp. 4057–4062.

[29] J.-H. Yoo, Maximization of hydropower generation through the application of a linear programming model, Journal of Hydrology 376 (1-2) (2009) 182–187.

[30] J. S. Anagnostopoulos, D. E. Papantonis, Flow Modeling and Runner Design Optimization in Turgo Water Turbines, International Journal of Mechanical, Aerospace, Industrial and Mechatronics Engineering 1 (4) (2007) 204–209.

[31] A. Tapia, D. G. Reina, P. Millán, An evolutionary computational approach for designing micro hydro power plants, Energies 12 (5) (2019) 878.

[32] A. Tapia, D. Reina, P. Millán, Optimized micro-hydro power plants layout design using messy genetic algorithms, Expert Systems with Applications (2020) 113539.

[33] J. S. Anagnostopoulos, D. E. Papantonis, Optimal sizing of a run-of-river small hydropower plant, Energy Conversion and Management 48 (10) (2007) 2663–2670.

[34] J. S. Anagnostopoulos, D. E. Papantonis, A fast Lagrangian simulation method for flow analysis and runner design in Pelton turbines, Journal of Hydrodynamics 24 (6) (2012) 930–941. doi:10.1016/S1001-6058(11)60321-1.
URL http://dx.doi.org/10.1016/S1001-6058(11)60321-1

[35] M. Ehteram, S. Binti Koting, H. A. Afan, N. S. Mohd, M. Malek, A. N. Ahmed, A. H. El-shafie, C. C. Onn, S. H. Lai, A. El-Shafie, New evolutionary algorithm for optimizing hydropower generation considering multireservoir systems, Applied Sciences 9 (11) (2019) 2280.

[36] K. V. Alexander, E. P. Giddens, Optimum penstocks for low head microhydro schemes, Renewable Energy 33 (3) (2008) 507–519. doi:10.1016/j.renene.2007.01.009.

[37] A. Tapia, P. Millán, F. Gómez-Estern, Integer programming to optimize micro-hydro power plants for generic river profiles, Renewable Energy 126 (2018) 905 – 914. doi:https://doi.org/10.1016/j.renene.2018.04.003.
URL http://www.sciencedirect.com/science/article/pii/S0960148118304105

[38] D. Whitley, A genetic algorithm tutorial, Statistics and computing 4 (2) (1994) 65–85.

[39] P. R. Green D., Perry's Chemical Engineers' Handbook, Eighth Edition, 2008.

[40] K. V. Alexander, E. P. Giddens, Microhydro: Cost-effective, modular systems for low heads, Renewable Energy 33 (6) (2008) 1379–1391. doi:10.1016/j.renene.2007.06.026.

[41] M. Arzamendia, D. Gregor, D. G. Reina, S. L. Toral, An evolutionary approach to constrained path planning of an autonomous surface vehicle for maximizing the covered area of ypacarai lake, Soft Computing 23 (5) (2019) 1723–1734.

[42] A. R. del Nozal, A. Tapia, L. Alvarado-Barrios, D. Reina, Application of genetic algorithms for unit commitment and economic dispatch problems in microgrids, in: Nature Inspired Computing for Data Science, Springer, 2020, pp. 139–167.

[43] D. E. Goldberg, J. H. Holland, Genetic algorithms and machine learning (1988).

[44] A. Ter-Sarkisov, S. Marsland, Convergence properties of two ({\mu}+{\lambda}) evolutionary algorithms on onemax and royal roads test functions, arXiv preprint arXiv:1108.4080 (2011).

[45] B. V. Cherkassky, A. V. Goldberg, T. Radzik, Shortest paths algorithms: Theory and experimental evaluation, Mathematical programming 73 (2) (1996) 129–174.

[46] S. Luke, Essentials of Metaheuristics, 2nd Edition, Lulu, 2013, available for free at http://cs.gmu.edu/~sean/book/metaheuristics/.

[47] K. Deb, A. Pratap, S. Agarwal, T. Meyarivan, A fast and elitist multiobjective genetic algorithm: Nsga-ii, IEEE transactions on evolutionary computation 6 (2) (2002) 182–197.

[48] T. A., Graph-based 3d mhpp ga, https://github.com/atapiaco/3DMHPP_GA/ (2021).

[49] C. Ingenieros, Generador de precios de la construcción (Honduras) (accessed 2021-03-01).
URL http://www.honduras.generadordeprecios.info/

Table B.6: Results of the tests proposed to tune p_{cx} and p_m

	Hyper-parameters					
p_{mut}	0.70	0.60	0.50	0.40	0.30	0.80
p_{cx}	0.30	0.40	0.50	0.60	0.70	0.20
	Final population fitness					
Mean	23163.58	23154.68	23089.08	23102.52	23068	23106.69
Std. dev.	126.18	379.38	533.74	692.18	974.91	1191.64
Min	22989.09	22991.07	22989.09	22989.09	22989.09	22989.09
Max	26626.23	56650.06	72280.29	60077.79	58350.76	60715.72
	Best individual					
Gross h. (m)	79.47	79.47	79.47	79.47	79.47	79.47
Power (W)	8055.57	8052.86	8055.57	8055.57	8055.57	8055.57
Pens. length (m)	521.49	522.21	521.49	521.49	521.49	521.49
Elbows	8	7	8	8	8	8
Pipe diam. (cm)	15	15	15	15	15	15
Cost (c.u.)	**22989.09**	**22991.07**	**22989.09**	**22989.09**	**22989.09**	**22989.09**

Table B.7: Results of the tests proposed to tune μ_{cx}

	Hyper-parameter				
μ_{cx}	0.20	0.40	0.50	0.60	0.80
	Final population fitness				
Mean	23121.37	23128.39	23163.58	23000.08	23084.31
Std. dev.	183.77	131.51	126.18	97.15	132.98
Min	22991.07	22999.37	22989.09	22989.09	22999.38
Max	37731.74	28299.79	26626.23	29467.18	29263.64
	Best individual				
Gross h. (m)	79.47	79.47	79.47	79.47	79.47
Power (W)	8052.86	8056.83	8055.57	8055.57	8056.83
Pens. length (m)	522.21	521.16	521.49	521.49	521.16
Elbows	7	7	8	8	7
Pipe diam. (cm)	15	15	15	15	15
Cost (c.u.)	**22991.07**	**22999.37**	**22989.09**	**22989.09**	**22999.38**

Table B.8: Results of the tests proposed to tune $p_{mut,mov}$

	Hyper-parameter				
$p_{mut,mov}$	0.01	0.05	0.10	0.15	0.20
	Final population fitness				
Mean	23085.53	23172.33	23030.18	23227.30	23276.39
Std. dev.	114.08	214.25	358.57	172.57	391.48
Min	22989.09	22989.09	22989.09	23109.34	22999.38
Max	28424.28	38428.53	58053.70	32309.88	58082.50
	Best individual				
Gross h. (m)	79.47	79.47	79.47	79.47	79.47
Power (W)	8055.57	8055.57	8055.57	8049.66	8056.83
Pens. length (m)	521.49	521.49	521.49	523.06	521.16
Elbows	8	8	8	7	7
Pipe diam. (cm)	15	15	15	15	15
Cost (c.u.)	**22989.09**	**22989.09**	**22989.09**	**23109.34**	**22999.38**

Table B.9: Results of the tests proposed to tune $p_{mut,10}$

	Hyper-parameter				
$p_{mut,10}$	0.01	0.05	0.10	0.15	0.20
	Final population fitness				
Mean	23666.23	23056.67	23126.67	23063.64	23110.79
Std. dev.	408.06	240.71	439.11	870.11	436.55
Min	23172.03	22989.09	22989.09	22991.07	22991.07
Max	26953.01	42658.04	62868.17	63565.87	56036.43
	Best individual				
Gross h. (m)	79.47	79.47	79.47	79.47	79.47
Power (W)	8033.66	8055.57	8055.57	8052.86	8052.86
Pens. length (m)	527.31	621.49	521.49	522.21	522.21
Elbows	11	8	8	7	7
Pipe diam. (cm)	15	15	15	15	15
Cost (c.u.)	**23172.03**	**22989.09**	**22989.09**	**22991.07**	**22991.07**

Table B.10: Results of the tests proposed to tune $p_{mut,10}$

	Hyper-parameter				
$p_{mut,10}$	0.01	0.05	0.10	0.15	0.20
	Final population fitness				
Mean	23179.04	23106.39	23104.00	23200.80	23093.56
Std. dev.	175.80	150.22	450.50	373.29	627.44
Min	22999.38	22991.07	22991.07	22991.07	22989.09
Max	28899.80	25997.63	66247.84	58437.92	61160.78
	Best individual				
Gross h. (m)	79.47	79.47	79.47	79.47	79.47
Power (W)	8056.83	8052.86	8052.86	8052.86	8055.57
Pens. length (m)	521.16	522.21	522.21	522.21	521.49
Elbows	7	7	7	7	8
Pipe diam. (cm)	15	15	15	15	15
Cost (c.u.)	**22999.38**	**22991.07**	**22991.07**	**22991.07**	**22989.09**